Patch-Clamp Recording of Charge Movement, Ca^{2+} Current, and Ca^{2+} Transients in Adult Skeletal Muscle Fibers

Zhong-Min Wang,* María Laura Messi,* and Osvaldo Delbono*#

*Department of Physiology and Pharmacology and #Department of Internal Medicine, Gerontology, Wake Forest University School of Medicine, Winston-Salem, North Carolina 27157 USA

ABSTRACT Intramembrane charge movement (Q), Ca^{2+} conductance (G_m) through the dihydropyridine-sensitive L-type Ca^{2+} channel (DHPR) and intracellular Ca^{2+} fluorescence (F) have been recorded simultaneously in flexor digitorum brevis muscle fibers of adult mice, using the whole-cell configuration of the patch-clamp technique. The voltage distribution of Q was fitted to a Boltzmann equation; the Q_{max}, $V_{1/2Q}$, and effective valence (z_Q) values were 41 ± 3.1 nC/μF, −17.6 ± 0.7 mV, and 2.0 ± 0.12, respectively. $V_{1/2G}$ and z_G values were −0.3 ± 0.06 mV and 5.6 ± 0.34, respectively. Peak Ca^{2+} transients did not change significantly after 30 min of recording. F was fit to a Boltzmann equation, and the values for $V_{F1/2}$ and z_F were 6.2 ± 0.04 mV and 2.4, respectively. F was adequately fit to the fourth power of Q. These results demonstrate that the patch-clamp technique is appropriate for recording Q, G_m, and intracellular [Ca^{2+}] simultaneously in mature skeletal muscle fibers and that the voltage distribution of the changes in intracellular Ca^{2+} can be predicted by a Hodgkin-Huxley model.

INTRODUCTION

The mechanism of excitation-contraction coupling (EC coupling) in skeletal muscle involves the sequential activation of the L-type Ca^{2+} channel $\alpha 1$ subunit and the sarcoplasmic reticulum Ca^{2+} release channel/ryanodine receptor (RyR1). The coupling between these two Ca^{2+} channels leads to elevations in myoplasmic Ca^{2+} concentration and subsequently to muscle contraction (Ashley et al., 1991; Schneider, 1994; Meissner, 1994). Because this system is triggered by changes in membrane voltage (Melzer et al., 1995), the simultaneous recording of sarcolemmal electrical properties and transient changes in intracellular Ca^{2+} concentration in single muscle fibers is essential for the understanding of EC coupling. Sarcolemmal membrane events and intracellular Ca^{2+} concentration have been recorded with the double vaseline gap technique in muscles from frog (for a review see Melzer et al., 1995) and rodents (Lamb, 1986; Delbono et al., 1995; Delbono and Stefani, 1993a,b; Garcia and Schneider, 1993; Szentesi et al., 1997; Shirokova et al., 1996). Although the vaseline-gap apparatus allowed for recording the function of the L-type Ca^{2+} channel-RyR1 interaction in mammalian muscle fibers, the studies in mammals (including humans) have been restricted to a few groups. An explanation for this could be the lack of more standard techniques available for assessing EC coupling in single mature skeletal muscle cells under voltage-clamp conditions. Another explanation could be the rapid rundown in the amplitude of the peak Ca^{2+} transient recorded in voltage-clamped cut fibers with the vaseline gap system. This prompted us to examine charge movement, calcium currents, and intracellular Ca^{2+} in adult skeletal muscle fibers with a more widely used electrophysiological technique such as the whole-cell configuration of the patch clamp (Hamill et al., 1981). This approach, used before for recording calcium currents in neonatal muscle fibers (Beam and Knudson, 1988; Gonoi and Hasegawa, 1988), has now been applied to the study of adult muscle fibers. Although this work has been focused on recording single mouse skeletal muscle fiber properties with the whole-cell configuration of the patch-clamp technique, experiments using the double vaseline gap voltage clamp have been performed when the information was not available in the literature.

In the present study we demonstrate that 1) the whole-cell configuration of the patch-clamp technique is appropriate for simultaneous recording of charge movement and/or calcium current and intracellular Ca^{2+} transients in flexor digitorum brevis muscle fibers of adult mice, 2) this technique provides experimental conditions for recording changes in the peak intracellular Ca^{2+} with negligible rundown, and 3) the voltage dependence of the peak intracellular Ca^{2+} follows the fourth power of the charge movement.

MATERIALS AND METHODS

Mouse skeletal muscle single fibers

Single skeletal muscle fibers from the flexor digitorum brevis (FDB) muscle were obtained from 5–7-month-old FVB mice raised in a pathogen-free area at the Animal Research Program of Wake Forest University School of Medicine (WFUSM). Animal handling and procedures followed an approved protocol by the Animal Care and Use Committee of WFUSM. FDB muscles were dissected in a solution containing 155 mM Cs-aspartate, 5 mM Mg-aspartate$_2$, 10 mM HEPES (pH 7.4 with CsOH) (Beam and Franzini-Armstrong, 1997). Muscles were treated with 2 mg/ml collagenase (Sigma, St. Louis, MO.) in a shaking bath at 37°C. After 3 h of enzymatic treatment, FDB muscles were dissociated into single fibers with Pasteur pipettes of different tip sizes.

Received for publication 27 May 1999 and in final form 26 July 1999.

Address reprint requests to Dr. Osvaldo Delbono, Department of Physiology and Pharmacology, Wake Forest University School of Medicine, Medical Center Boulevard, Winston-Salem, NC 27157. Tel.: 336-716-9802. Fax: 336-716-2273; E-mail: odelbono@wfubmc.edu.

0006-3495/99/11/2709/08 $2.00

Charge movement and calcium current recordings

Muscle fibers were transferred to a small flow-through Lucite chamber positioned on a microscope stage. Fibers were continuously perfused with the external solution (see below), using a push-pull syringe pump (WPI, Saratoga, FL). Only fibers exhibiting a clean surface and lack of evidence of contracture were used for electrophysiological recordings. Muscle fibers were voltage-clamped using an Axopatch-200B amplifier (Axon Instruments, Foster City, CA) in the whole-cell configuration of the patch-clamp technique (Hamill et al., 1981). Patch pipettes were pulled from borosilicate glass (Boralex), using a Flaming Brown micropipette puller (P97; Sutter Instrument Co., Novato, CA) and then fire-polished to obtain an electrode resistance ranging from 450 to 650 kΩ. In cell-attached configuration the seal resistance was in the range of 400 MΩ to 4.5 GΩ ($n = 50$), and in the whole-cell configuration the values were between 75 and 120 MΩ. Only experiments with resistance more than 75 MΩ were included in the analysis. The pipette was filled with the following solution (mM): 140 Cs-aspartate; 2 Mg-aspartate$_2$, 0.2 or 10 Cs_2EGTA, and 10 HEPES, with pH adjusted to 7.4 with CsOH (Adams et al., 1990; Wang et al., 1999). The external solution used for Ca^{2+} current recording contained (in mM) 150 TEA (tetraethylammonium hydroxide)-CH_3SO_3, 2 $MgCl_2$, 2 $CaCl_2$, 10 Na-HEPES, and 0.001 tetrodotoxin (Delbono, 1992; Delbono et al., 1997). Solution pH was adjusted to 7.4 with CsOH. Both the pipette and the bath solution were selected based on the ease of membrane seal formation and cell stability over time. For charge movement recording, Ca^{2+} current was blocked with the external solution containing 0.5 mM Cd^{2+} and 0.3 mM La^{3+} (Adams et al., 1990; Wang et al., 1999).

Whole-cell currents were acquired and filtered at 5 kHz with pCLAMP 6.04 software (Axon Instruments). A Digidata 1200 interface (Axon Instruments) was used for A-D conversion. Membrane current during a voltage pulse, P, was initially corrected by analog subtraction of linear components. The remaining linear components were digitally subtracted on-line, using hyperpolarizing control pulses of one-quarter test pulse amplitude ($-P/4$ procedure) (Bezanilla, 1985; Delbono, 1992) as described for rat and mouse muscle fibers (Delbono, 1992; Delbono et al., 1997). Four control pulses were applied before the test pulse. Charge movements were evoked by 25-ms depolarizing pulses from the holding potential (−80 mV) to command potentials ranging from −70 to 70 mV with 10-mV intervals. Intramembrane charge movement was calculated as the integral of the current in response to depolarizing pulses (charge on, Q_{on}) and is expressed per membrane capacitance (coulombs per farad). The complete blockade of the inward Ca^{2+} current was verified by the Q_{on}-Q_{off} linear relationship.

Extensor digitorum longus (EDL) muscle fibers were manually dissociated from adult FVB mice (5–7 months old) and voltage-clamped using the double vaseline gap technique and solutions previously described (Delbono, 1992; Delbono et al., 1997).

Intracellular Ca^{2+} transient recording

Intracellular Ca^{2+} transients were recorded simultaneously with sarcolemmal currents in single voltage-clamped FDB muscle fibers. In this group of experiments the pipette solution contained 0.2 mM EGTA. A group of experiments done in 0.05 and 0.1 mM EGTA did not show significant changes in the intracellular Ca^{2+} transient kinetics (data not shown). Three fluorescent indicators (fluo-3, calcium green-5N, and calcium orange-5N; Molecular Probes, Eugene, OR) with different affinity for Ca^{2+} were used (see below). The fibers were loaded with the Ca^{2+} dye via the patch pipette. After whole-cell voltage clamp was attained, the dye was allowed to diffuse for 20–30 min before the fiber was pulsed. This time is similar to that used for loading EDL fibers in the double vaseline gap chamber. For fluorescent recordings, the fiber was illuminated with a 75-W xenon lamp through a 20× Fluar objective (Zeiss, Oberkochen, Germany). The light beam passed through selectable 485 (fluo-3 or calcium green-5N) or 550 nm (calcium orange-5N) excitation wavelength filters with a 10-nm bandwidth (Omega Optical, Brattleboro, VT) mounted in a computer-controlled filter wheel (Ludl Electronics, Hawthorne, NY). The light was reflected by a dichroic mirror centered at 505 nm (DRLPO2; Omega Optical) (fluo-3 and calcium green-5N) and 575 nm (DRLPO2; Omega Optical) (calcium orange-5N) at a 45° angle. The emitted light was collected by a frame-transferred CCD camera (PXL-EEV-37; Photometrics, Tucson, AZ) after passing through emission filters centered at 535 nm (DF35) and 615 nm (DF45) (Omega Optical) for fluo-3 or calcium green-5N and calcium orange-5N, respectively. Hardware control, image acquisition, and processing were done with ISee software (Inovision, Durham, NC) run in a SUN (Mountain View, CA) or a Silicon Graphics O_2 (Mountain View, CA) workstation. Although the fluorescence was recorded from the whole cell, only a rectangular region of interest (ROI) of ~2000–3000 pixels near the patch pipette was analyzed. The patch pipette was not included in the ROI. Mean values of fluorescence changes corrected to basal fluorescence were plotted over time. Sequences of images for up to 2 s were acquired at 50 frames/s (20-ms interval). All of the records were corrected for background fluorescence (optical pathway) and photobleaching. Data are expressed as a percentage of change in fluorescence normalized to basal fluorescence ($\%\Delta F/F$) (Finch and Augustine, 1998).

Ca^{2+} indicator calibration

The dissociation constant (K_d) for Ca^{2+} of the fluorescent indicators was determined by measuring the saturation curve in vitro at pCa (−log [Ca^{2+}]) ranging from 8 to 1. The Ca^{2+} indicator was diluted in calibration solutions (CAL-BUF-1 and CAL-BUF-2; WPI) to a final concentration of 100 μM. Aliquots (3 μl) were placed on the chamber used for muscle fiber recording. Values were normalized to the maximum fluorescence and fitted to an equation of the form

$$y = 1/(1 + (K_d/[Ca^{2+}])). \quad (1)$$

The K_d was determined in the same lot of the dyes used for the studies in muscle fiber, and the values for fluo-3, calcium green-5N, and calcium orange-5N were 849 nM, 33 μM, and 55 μM, respectively ($n = 5$ for each dye).

All of the experiments were carried out at room temperature (22°C). Data values are given as means ± SEM with the number of observations (n). Experimental groups have been statistically analyzed using Student's pair or unpaired t-test, and $p < 0.05$ was considered significant.

RESULTS

Membrane properties of FDB muscle fibers

Fiber capacitance was calculated from the integral of the capacitive transient current elicited by 10-mV hyperpolarizing pulses from the holding potential of −80 mV (Fig. 1 *A*). The FDB muscle fibers used in this work are smaller than the fragments of mouse or rat EDL muscle fibers used in the vaseline gap voltage clamp. The capacitance of the FDB fibers was 1680 ± 123 pF (range: 868-2419 pF; $n = 32$). The input capacitance of rat and mouse fiber segments used for the double vaseline gap voltage-clamp technique was 5514 ± 241 pF ($n = 39$) and 4216 ± 312 pF ($n = 27$), respectively. The length and diameter of the FDB fibers were 462 ± 16 μm (range: 385–500) and 33 ± 1.7 μm (range: 25–39; $n = 32$), respectively. The length of the rat and mouse EDL fibers mounted in the double vaseline system was 1.1 mm (central pool plus the area under the vaseline seals) and was determined by the chamber's design. The diameter of the EDL fibers was 45 ± 3.5 ($n = 39$) and 36 ± 4.7 μm ($n = 27$), respectively. The time constant

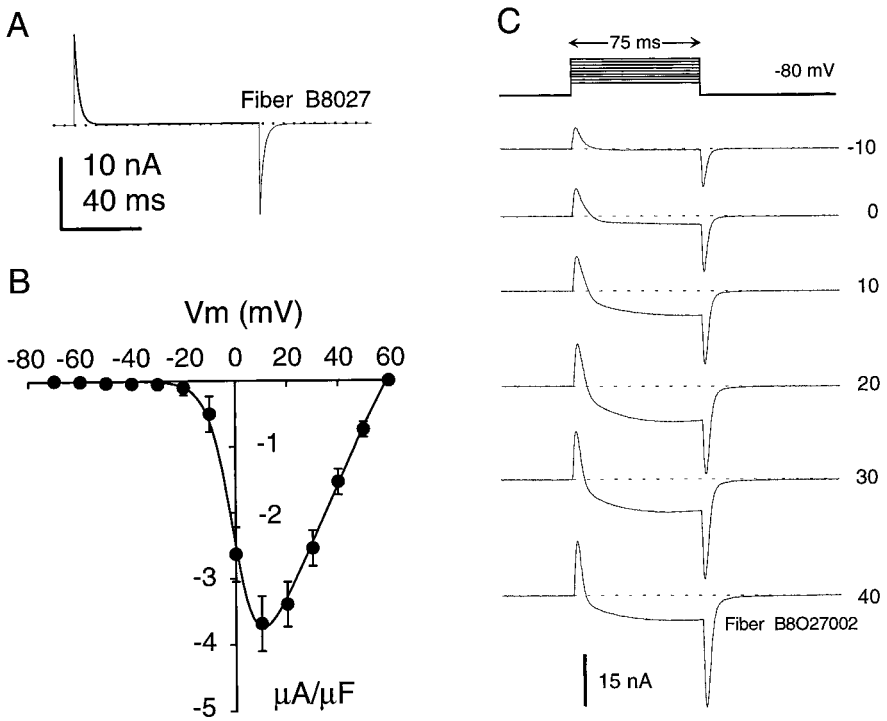

FIGURE 1 (*A*) Capacity current recorded in a FDB muscle fiber recorded with the whole-cell configuration of the patch-clamp technique. The record illustrates a typical capacity current (*thin continuous line*) evoked by a hyperpolarizing pulse from the holding potential (−80 mV) to a command pulse of −90 mV. The time constant of the current relaxation was fitted to a first-order exponential function (τ = 1.1 ms) plus a constant (*thick line*). (*B*) Ca^{2+} current-voltage relationship. Ca^{2+} currents evoked by 75-ms pulses from the holding potential (−80 mV) to depolarizing command pulses from −70 to 60 mV are shown. Experimental data were fitted to Eq. 3 (*continuous line*). Data points represent the mean ± SEM of 30 muscle fibers. (*C*) Slow inward Ca^{2+} current. Selected traces evoked by command pulses of 75 ms duration from −10 to 40 mV are depicted. The discontinuous line in *A* and *C* represents the baseline.

of the current relaxation was fitted to a first-order exponential function plus a constant in all of the cells studied (n = 32). The capacity currents recorded in EDL mouse or rat fibers with the vaseline gap technique were fitted to a one- or two-order exponential function according to the fiber diameter. A single-exponential capacity current consistently correlated with fibers with a diameter of 50 ± 3.8 μm or less (n = 56). The apparent series or access resistance (R_a) was measured by potentiometric adjustment of the patch-clamp amplifier and corrected according to the following equation:

$$R_a = V/((V/R_x) + \sum W_i), \quad (2)$$

where V is the membrane voltage, R_x is the apparent access resistance (directly measured by potentiometric series resistance compensation), and W_i is the sum of the amplitudes of the time constants used for fitting the decaying phase of the capacity current (Jackson, 1992). The mean R_a value was 0.58 ± 0.02 MΩ, and the range was 0.42–0.75 MΩ (n = 30). The values for mouse EDL fibers voltage-clamped with the double vaseline gap apparatus were 0.14 ± 0.03 MΩ (range = 0.08–0.34 MΩ; n = 25).

Calcium current

The dihydropyridine-sensitive slow inward Ca^{2+} current was recorded, using Ca^{2+} as the charge carrier. The composition of the bath solution was the same used for studies in rat, human, and mouse adult muscle fibers voltage-clamped in the double vaseline-gap apparatus (Delbono, 1992; Delbono et al., 1995, 1997). The pipette solution used in these experiments is the one used for recording in primary cultured rat myoballs (Wang et al., 1999). The combination of these two solutions facilitated the gigaohm seal formation and the stability of the preparation. The current traces were capacity compensated such that only charge movement contributes to the initial outward current. Ca^{2+} currents were evoked by 75-ms depolarizing steps from the holding potential ([minus80 mV) to command potentials ranging from −70 to 50 mV. Ca^{2+} current was activated at a potential ranging from −40 to −20 mV and reached a peak between 10 and 20 mV, to decline in amplitude at more positive potentials. The onset of the current was slow and reached a plateau at ~50 ms after the beginning of the pulse. Fig. 1, *B* and *C*, shows the current-voltage relationship from −70 to 60 mV and representative Ca^{2+} current traces from −10 to 40 mV. Ca^{2+} currents reach a peak of 3.7 ± 0.45 μA/μF at 15 ± 0.9 mV (n = 30). The inward Ca^{2+} current (I_{Ca}) was fit to the following equation:

$$I_{Ca} = G_{max}(V - V_r)/\{1 + \exp[zF(V_{1/2} - V)/RT]\}, \quad (3)$$

where G_{max} is the maximum conductance, V is the membrane potential, V_r is the reversal potential, $V_{1/2}$ is the half-activation potential, z is the effective valence, F is the Faraday constant, R is the gas constant, and T is the absolute temperature (296 K) (Delbono et al., 1997). The G_{max}, $V_{1/2}$, V_r, and z values calculated from the fitting to individual experiments are 85 ± 4.3 nS/nF, −0.3 ± 0.06 mV, 59.4 ± 1.2 mV, and 5.6 ± 0.34 (n = 32), respectively.

Charge movement

Fig. 2 *A* shows a group of charge movement traces in response to 25-ms depolarizing voltage steps from the hold-

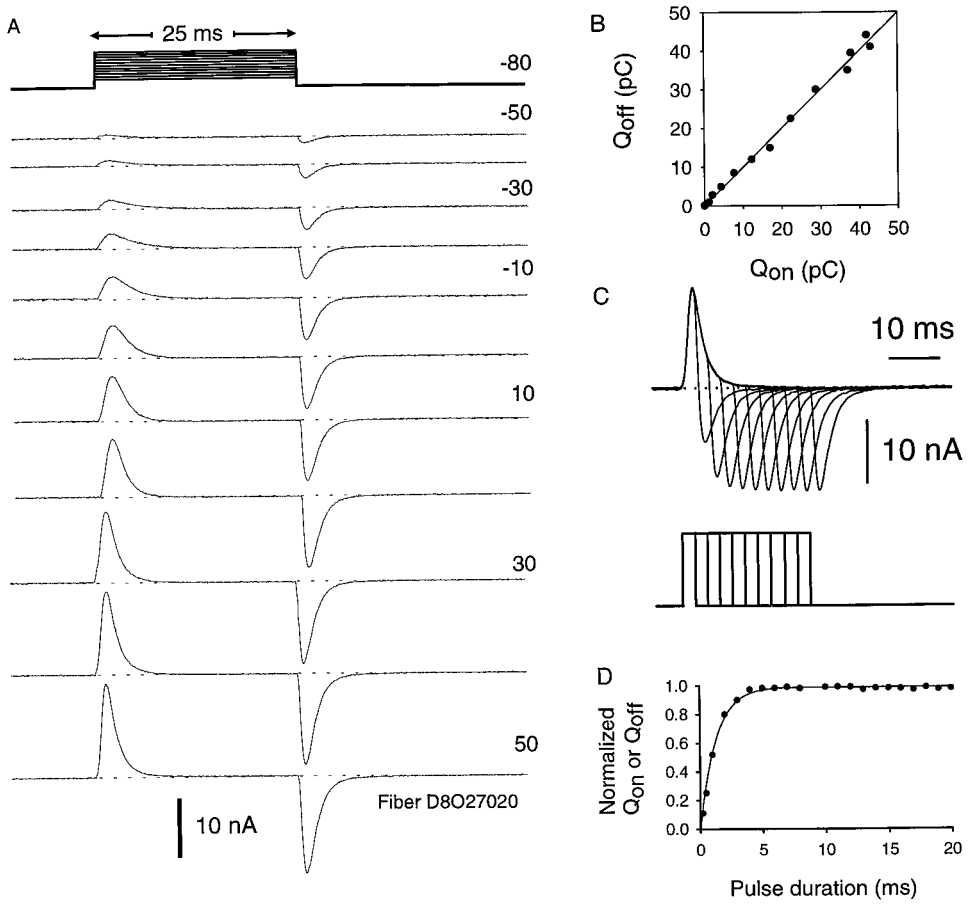

FIGURE 2 (*A*) Charge movement in adult FDB muscle fibers. Charge movement was recorded after the inward Ca^{2+} current was blocked with a mixture of 0.5 mM Cd^{2+} and 0.3 mM La^{3+} added to the external solution. Charge movement was evoked by 25-ms depolarizing voltage steps from the holding potential (−80 mV) to the command potentials ranging from −50 to 50 mV. The discontinuous line represents the baseline. (*B*) Linear Q_{on}-Q_{off} relationship. The complete blockade of the inward Ca^{2+} current was demonstrated by the equal charge moved during the depolarization (Q_{on}) and repolarization (Q_{off}) (linear Q_{on} versus Q_{off} relationship) (fiber D8O$_2$7020; see Fig. 2 *A*). (*C*) Charge movement conservation. Charge movement conservation was recorded in response to depolarizing pulses to 20 mV of different duration (1.5 ms with 1.5-ms increments). The pulse protocol is shown at the bottom. (*D*) Complete set of pulses corresponding to the muscle fiber illustrated in *A* and *C*. The normalized charge-pulse duration relationship was fit to a single exponential equation (Eq. 4) (*continuous line*).

ing potential (−80 mV) to the command potentials ranging from −50 to 50 mV. Fig. 2, *B–D*, shows that the current recorded after the inward Ca^{2+} current is blocked is the intramembrane charge movement, because it shows saturation at both extremes of the voltage range, and the amount of charge moved during depolarization (Q_{on}) is equal to the charge that returns during the repolarization (Q_{off}). Fig. 2 *B* shows that the inward Ca^{2+} current was completely blocked, and the amount of charge moved during the depolarization (Q_{on}) is equal to the charge moved during repolarization (Q_{off}), as demonstrated by the linear Q_{on} versus Q_{off} relationship for each command pulse (fiber D8O$_2$7020; Fig. 2 *A*). Fig. 2 *C* shows the charge movement conservation in response to 10 depolarizing pulses to 20 mV of different duration (1.5 ms with 1.5-ms increments). Fig. 2 *D* shows the complete set of pulses corresponding to the same muscle fiber. The normalized charge-pulse duration relationship was fit to a single exponential function (continuous line) of the form

$$y = a^*(1 - \exp(-x/\tau)), \quad (4)$$

The calculated time constant (τ) value was 1.28 ms.

Intracellular Ca^{2+} transients

Transient increases in intracellular Ca^{2+}, evoked by changes in membrane voltage were recorded using fluo-3, calcium green-5N, or calcium orange-5N as Ca^{2+} indicators. Fig. 3 illustrates the simultaneous recording of membrane current (Fig. 3 *A*) and Ca^{2+} transients using fluo-3 (Fig. 3 *B*). Cell response was evoked by command depolarizations from −10 to 30 mV. Membrane currents and Ca^{2+} fluorescence have been illustrated on a time scale that allows display of the complete records. The analysis of the normalized fluorescence values between 10 and 50 mV did not show statistical significant differences. In a separate group of experiments, changes in intracellular fluorescence were recorded using calcium green-5N as a Ca^{2+} fluorescent probe (Fig. 3 *C*). The calcium transients recorded with calcium green-5N decay on a faster time scale than those recorded with fluo-3, as expected for a relatively low-affinity Ca^{2+} indicator (K_d = 33 μM). This is illustrated in Fig. 3 *D*, where superimposed traces of intracellular Ca^{2+} transients recorded with fluo-3 and calcium green-5N are shown. Although records with calcium green-5N show a faster decay, the traces do not reach the baseline (*dotted line*), as expected for a relatively low-affinity Ca^{2+} indicator. To determine whether the slow relaxation phase can be ascribed to physical properties of the dye, the buffer capacity of the cells, or the technical procedures employed, the low-affinity Ca^{2+} indicator calcium orange-5N (K_d = 55 μM) was used. As shown in Fig. 3 *D*, the complete return of the Ca^{2+} transient recorded with calcium orange-5N to the baseline allows us to rule out technical procedures and

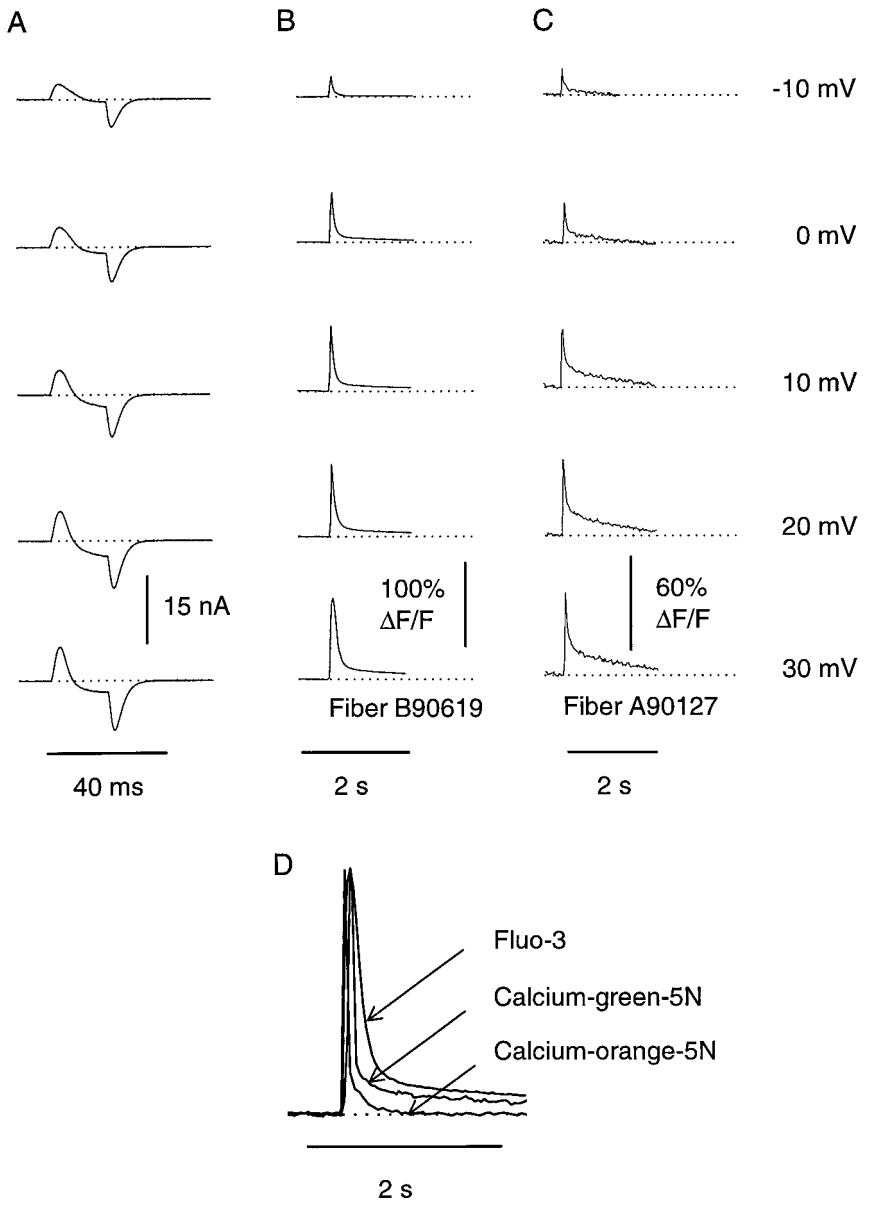

FIGURE 3 Membrane currents and intracellular Ca^{2+} recordings in FDB muscle fibers. (*A*) Charge movement and inward Ca^{2+} current. (*B*) Intracellular Ca^{2+} transients recorded with the Ca^{2+} indicator fluo-3 from −10 to 30 mV. (*C*) Membrane currents and intracellular Ca^{2+} recording with in FDB muscle fibers. Intracellular Ca^{2+} transients were recorded with calcium green-5N from −10 to 30 mV. (*D*) Calcium green-5N and calcium orange-5N fluorescence emission normalized to fluo-3 maximum fluorescence emission and superimposed. The discontinuous line represents the baseline.

cell buffer capacity as plausible explanations. Although the origin of the slow decay phase of the Ca^{2+} transient monitored with calcium green-5N is not known, it has been postulated that the broad half-width of the fluorescent signal is not related to heavy saturation of the indicator with Ca^{2+}. Some physical properties of calcium green-5N upon binding to Ca^{2+} have been discussed (see Zhao et al., 1996). The analysis of the Ca^{2+} transients also showed that the rising phase was faster when calcium orange-5N was used (3.2 ± 0.3 ms) instead of calcium green-5N (5.1 ± 0.2 ms) or fluo-3 (6.8 ± 0.4 ms).

Repetitive measurements of Q_{max}, C_i, Ca^{2+} current, and Ca^{2+} fluorescence

Fig. 4 shows the time course of repetitive measurements (every 5 min) of the normalized maximum charge movement, membrane capacitance, Ca^{2+} current, and peak Ca^{2+} transient recorded with calcium green-5N. The charge movement, as a capacitive current, follows the time course of the membrane capacitance. For these experiments, fibers were voltage-clamped at $V_h = -80$ mV for 20 min, allowing the dye to diffuse. Similarly, EDL fibers were voltage-clamped at $V_h = -80$ mV, using the double vaseline gap apparatus, and allowed to equilibrate for 25–30 min with the dye. After this period we began to pulse the fiber (time 0). Ca^{2+} current and intracellular Ca^{2+} transients were recorded simultaneously by applying single depolarizing pulses to 20 mV every 5 min. Charge movement and membrane capacity were recorded in a separate group of experiments in response to the pulse protocols described above. For these experiments the cells were not loaded with the dye. Q_{max} (*circles*), C_m (*up triangles*), and Ca^{2+} current (I_{Ca}) (*squares*) declined to 0.85 ± 0.04, 0.88 ± 0.03, and 0.78 ± 0.04 ($n = 15$, $p > 0.05$) of their initial value, respectively, at 30 min of current recording. The peak Ca^{2+}

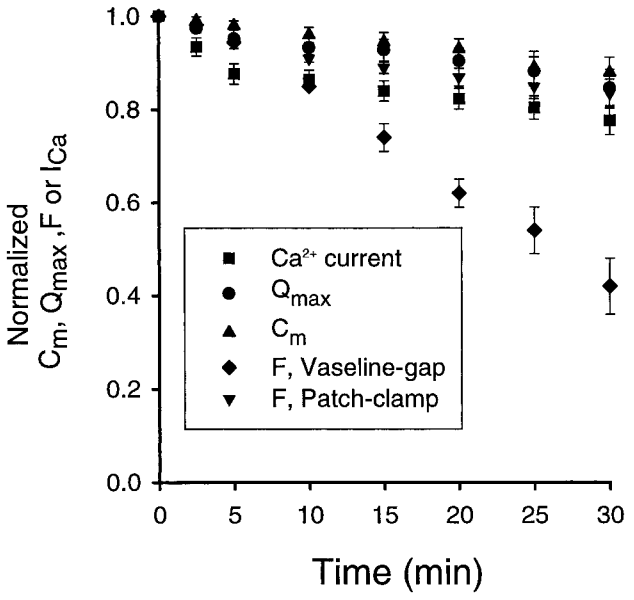

FIGURE 4 Repetitive measurements of the normalized C_m, Q_{max}, Ca^{2+} current, or Ca^{2+} fluorescence in FDB and EDL muscle fibers. Membrane capacitance (C_m) (▲), maximum charge movement (Q_{max}) (●), peak calcium current (I_{Ca}) (■) amplitude, and intracellular peak Ca^{2+} transient (F) recorded with calcium green-5N in FDB mouse fibers (▼) were monitored for 30 min. Intracellular Ca^{2+} fluorescence was recorded in EDL fibers, using calcium green-5N and the double vaseline gap technique (rhomboids).

transient amplitude recorded with fluo-3 or calcium green-5N (*down triangles*) at 30 mV was monitored every 5 min for 30 min. The ratio between the peak Ca^{2+} transient amplitude at 30 min and the peak Ca^{2+} transient at time 0 was 0.92 ± 0.11 (n = 25). The similar time courses of Q_{max}, C_m, Ca^{2+} current, and Ca^{2+} fluorescence indicate that detubulation results in changes in the amount of charge movement. These results were compared with the time courses of Q_{max}, C_m, I_{Ca}, and F (rhomboids) recorded in mouse EDL muscle fibers with the cut-fiber voltage-clamp procedure, using the same experimental protocols. Q_{max}, C_m, I_{Ca}, and F values at 30 min over the records at time 0 were 0.88 ± 0.03, 0.86 ± 0.05, 0.75 ± 0.04, and 0.43 ± 0.08, respectively (n = 25). Statistical analysis of these results shows that the decline in the peak Ca^{2+} fluorescence recorded using the vaseline gap technique and the difference between these values and those recorded by the whole-cell patch-clamp method are significant ($p < 0.01$). Statistical analysis of Q_{max}, C_m, and Ca^{2+} current recorded with the double vaseline gap voltage-clamp technique and comparison with the results obtained with the other technique were not significant. These data indicate that the electrical properties of the sarcolemma are similarly preserved with either the whole-cell patch-clamp or the Vaseline gap voltage-clamp; however, the sarcoplasmic reticulum Ca^{2+} release is better maintained when the former technique is used. A plausible explanation for this would be that the area of cellular access is significantly larger in the cut muscle fiber, allowing for an almost free diffusion of cytoplasmic components into the lateral pools.

Comparison of the voltage dependence charge movement, Ca^{2+} conductance, and intracellular Ca^{2+} fluorescence

Fig. 5 compares the voltage dependence of Q_{on} (*circles*), G_m (Ca^{2+} conductance) (*triangles*), and Ca^{2+} fluorescence recorded with calcium green-5N (*squares*) from −70 to 60 mV. For the analysis of the voltage dependence of Q, the data points were fitted to a Boltzmann equation of the form

$$Q_{on} = Q_{max}/\{1 + \exp[z_Q F(V_{1/2Q} - V_m)/RT]\}, \qquad (5)$$

where Q_{max} is the maximum charge, V_m is the membrane potential, $V_{1/2Q}$ is the charge movement half-activation potential, z_Q is the effective valence, and F, R, and T have their usual thermodynamic meanings. The Q_{max}, $V_{1/2Q}$, and z_Q values from the analysis of individual experiments were 41 ± 3.1 nC/μF, −17.6 ± 0.7 mV, and 2.0 ± 0.12, respectively. The F-V relationship (*squares*) was fitted to a Boltzmann equation (Eq. 5) and exhibited a voltage dependence similar to that of the intramembrane charge movement (*circles*) but different from that of the G-V relationship (*triangles*). The F-V relationship recorded with calcium green-5N was similar to that recorded with fluo-3. Increases in intracellular Ca^{2+} were detected between −30 and −20 mV and saturated at 20–30 mV, and the $V_{1/2F}$ (Ca^{2+} fluorescence half-activation potential) was 6.2 ± 0.04 and 5.1 ± 0.06 mV for fluo-3 and calcium green-5N, respectively. As charge movement and intracellular Ca^{2+} have been studied simultaneously in FDB fibers, we examined whether the voltage dependence of the charge and intracellular Ca^{2+} fluorescence exhibits a relationship similar to that described for frog muscle fibers (Simon and Hill, 1992). To this end, the F-V relationship was fitted to the Q-V relationship elevated to the fourth power ($Q^4(V)$) (Fig. 5, *dotted line*).

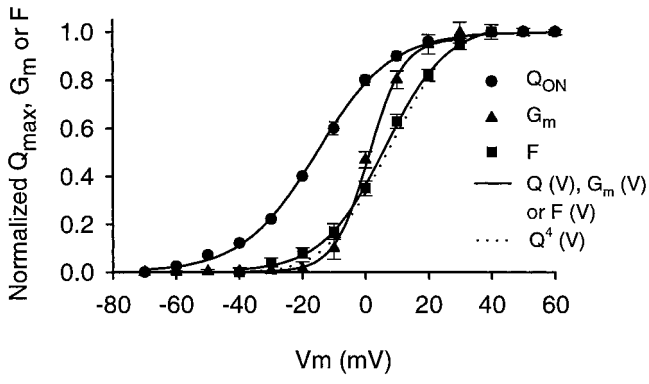

FIGURE 5 Voltage dependence of charge movement (Q), Ca^{2+} conductance (G_m), and intracellular Ca^{2+} fluorescence (F) in FDB muscle fibers recorded with the whole-cell configuration of the patch-clamp technique and calcium green-5N as a calcium indicator. Experimental data have been fitted to Eq. 5 for $Q_{on}(V)$ and $F(V)$ and to Eq. 3 for $G_m(V)$ (*continuous line*). The F-V relationship was also fitted to $Q^4(V)$. Values are mean ± SEM.

DISCUSSION

In this study we demonstrate the feasibility of the simultaneous recording of charge movement and/or slow Ca^{2+} current together with intracellular Ca^{2+} (with low- and high-affinity fluorescent Ca^{2+} indicators) mature skeletal muscle fibers, using the whole-cell configuration of the patch-clamp technique. We also show that this preparation allows for a more stable recording of intracellular Ca^{2+} and that the voltage dependence of the elevations in intracellular Ca^{2+} ($F(V)$) follows a relation with the voltage dependence of the charge movement ($Q(V)$) similar to that described for frog muscle fibers (Simon and Hill, 1992).

Comparison of membrane currents recorded in adult mammalian skeletal muscle fibers with different voltage-clamp techniques

Two methods have been successfully applied to the recording of Ca^{2+} current and intramembrane charge movement in adult mammalian skeletal muscle fibers, the microelectrode, and the double vaseline-gap voltage-clamp technique (Hollingworth and Marshall, 1981; Dulhunty and Gage, 1983; Delbono, 1992; Lamb, 1986). Q_{max}, $V_{1/2Q}$, and K (steepness of $Q(V)$) recorded with the middle of the fiber microelectrode technique in rat EDL muscle fibers ranged from 23 to 46 nC/μF, −18 to −34 mV, and 8.7 to 13.4, respectively (Hollingworth and Marshall, 1981; Simon and Beam, 1985; Hollingworth et al., 1990). Q_{max} and K values are similar to the values reported here, but $V_{1/2Q}$ is more negative (41 ± 3.1 nC/μF and 7.3 ± 0.6, −17.6 ± 0.7 mV, respectively). Q_{max}, $V_{1/2Q}$, and K have been recorded in rat fast-twitch muscle fibers with the double or triple vaseline gap voltage clamp. K and Q_{max} values measured in rat fibers with the triple (15.3 and 25.4 nC/μF, respectively) or the double (11.9 and 15.4 nC/μF, respectively) vaseline gap technique are similar to the values reported in the present work. However, $V_{1/2Q}$ measured with both the triple and double vaseline gap apparatus (−26.8 and −25.2 mV, respectively) (Delbono, 1992; Lamb, 1986; Lamb and Walsh, 1987) were more negative than the values reported here. Voltage clamp of mouse EDL muscle fibers with the same variant of the vaseline gap technique showed Q_{max} and $V_{1/2Q}$ values similar to those recorded in rat EDL fibers but different from those recorded with the whole-cell patch clamp. This difference resides on a smaller Q_{max} and more negative distribution of the charge (Delbono et al., 1997). Charge movement has been recorded in human quadriceps muscle fibers with the double vaseline gap technique (Garcia et al., 1992; Delbono et al., 1995). Although Q_{max}, $V_{1/2Q}$, and K values (5.2 nC/μF, −45.9 mV, and 12.9) are similar to those recorded in EDL fiber with the same technique, they differ significantly from those reported in the present work. Inherent differences in the voltage-clamp method, solutions, and muscle fiber subtype employed could be some of the explanations for this discrepancy. Among the differences in the voltage-clamp method, it should be considered that a less polarized membrane under the vaseline seals might contribute to the shift in the Q-V relationship in the voltage axis (Chandler and Hui, 1990).

The dihydropyridine-sensitive Ca^{2+} current has been recorded in adult mouse and rat skeletal muscle fibers with the vaseline gap technique. The peak Ca^{2+} current in this work is intermediate between the values recorded with the double vaseline gap (4.8 μA/μF, 0 mV) (Delbono, 1992) and the triple vaseline gap (1.5 A/F, 10–20 mV) (Lamb and Walsh, 1987). G_{max} is similar to that recorded in mouse EDL muscle fibers studied with the double vaseline gap voltage clamp (55 ± 6.3 nS/nF) (Delbono et al., 1997). The half-activation potential ($V_{1/2}$) in this work (−0.3 mV) differs from the value reported for mouse (−18.8 mV) and rat (−4.4 mV) fibers recorded with the double vaseline apparatus (Delbono, 1992; Delbono et al., 1997). The big pipette tip variant of the whole-cell configuration of the patch-clamp technique has been used for recording Ca^{2+} current in skeletal muscle fibers, but only in the postnatal period; however, charge movement has not been reported with this technique previously (Gonoi and Hasegawa, 1988). It should be noticed that the low resistance seal between the glass pipette or the vaseline and the sarcolemma, together with the substantial t-tubule present in adult fibers, limits the speed of the voltage clamp (Simon and Beam, 1985).

Comparison of intracellular Ca^{2+} recorded in adult mammalian skeletal muscle fibers with different voltage-clamp techniques

Although SR Ca^{2+} release is graded by sarcolemmal voltage, very little is known about the interdependence of charge movement, Ca^{2+} current, and SR Ca^{2+} release in adult mammalian skeletal muscle fibers. Two other techniques have been used to record changes in intracellular Ca^{2+} in mature mammalian skeletal muscle under voltage clamp, the double vaseline gap, and the silicone-embedded fiber techniques (Delbono and Stefani, 1993a,b; Garcia and Schneider, 1993; Delbono and Meissner, 1995; Shirokova et al., 1996; Jacquemond, 1997). However, in none of these works have Q or G_m and F been measured simultaneously. An explanation for this could be that the holding current in contracting cells is higher than in fibers voltage-clamped in high intracellular EGTA. In the present work, Ca^{2+} current, charge movement, and intracellular Ca^{2+} have been recorded in the same mouse muscle fiber because the whole-cell configuration of the patch-clamp technique allows for more stable recording conditions.

G_m and F have been recorded in cultured myotubes, using the whole-cell configuration of the patch clamp, and $G(V)$ was found more positive than $F(V)$ (Garcia and Beam, 1994). These results differ from those reported in the present study in that $F(V)$ (recorded with calcium green-5N) and $G(V)$ do not differ significantly from −30 to 0 mV, and F becomes more positive than G at voltages more positive than 10 mV. The z values for F and G are 2.4 and 5.6,

respectively (the z value for F recorded with fluo-3 was 2.1). Unfortunately, a comparison between the two works is difficult because of the different pulse protocol used. Garcia and Beam (1994) used brief depolarizations (pulse duration 15 ms) that led to an incomplete activation of the slow Ca^{2+} current. This is in contrast to the longer pulse protocol (70 ms) used here, which allowed a steady-state activation of the current. Furthermore, the Ca^{2+} concentration in the recording solution and stage of cell development differed between the two works.

Based on the similar F and Q voltage dependence in FDB fibers reported here, we attempted to determine whether $F(V)$ follows a relation to $Q(V)$ similar to that described for frog muscle fibers (Simon and Hill, 1992). $F(V)$ was well fit by the fourth power of charge movement, as predicted by a Hodgkin-Huxley (H-H) model with four particles (Hodgkin and Huxley, 1952). This is consistent with both morphological studies (Block et al., 1988) and physiological analysis (Simon and Hill, 1992), which support the concept that activation of sarcoplasmic reticulum Ca^{2+} release is controlled cooperatively by four dihydropyridine receptors.

This work was supported by National Institutes of Health/National Institute on Aging grants AG00692, AG13934, AG10484, and AG15820 to OD.

REFERENCES

Adams, B. A., T. Tanabe, A. Mikami, S. Numa, and K. G. Beam. 1990. Intramembrane charge movement restored in dysgenic skeletal muscle by injection of dihydropyridine receptor cDNAs. *Nature.* 346:569–572.

Ashley, C. C., I. Mulligan, and J. L. Trevor. 1991. Ca^{2+} and activation mechanisms in skeletal muscle. *Q. Rev. Biophys.* 24:1–73.

Beam, K. G., and C. Franzini-Armstrong. 1997. Functional and structural approaches to the study of excitation-contraction coupling. *Methods Cell Biol.* 52:283–306.

Beam, K. G., and C. M. Knudson. 1988. Calcium currents in embryonic and neonatal mammalian skeletal muscle. *J. Gen. Physiol.* 91:781–798.

Bezanilla, F. 1985. Gating of sodium and potassium channels. *J. Membr. Biol.* 88:97–111.

Block, B. A., T. Imagawa, K. P. Campbell, and C. Franzini-Armstrong. 1988. Structural evidence for direct interaction between the molecular components of the transverse tubule/sarcoplasmic reticulum junction in skeletal muscle. *J. Cell. Biol.* 107:2587–2600.

Chandler, W. K., and C. S. Hui. 1990. Membrane capacitance in frog cut twitch fibers mounted in a double vaseline-gap chamber. *J. Gen. Physiol.* 225–256.

Delbono, O. 1992. Calcium current activation and charge movement in denervated mammalian skeletal muscle fibers. *J. Physiol. (Lond.).* 451: 187–203.

Delbono, O. 1995. Ca^{2+} modulation of sarcoplasmic reticulum Ca^{2+} release in rat skeletal muscle fibers. *J. Membr. Biol.* 146:91–99.

Delbono, O., K. S. O'Rourke, and W. H. Ettinger. 1995. Excitation-calcium release uncoupling in aged single human skeletal muscle fibers. *J. Membr. Biol.* 148:211–222.

Delbono, O., M. Renganathan, and M. L. Messi. 1997. Regulation of mouse skeletal L-type Ca^{2+} channel by activation of the insulin-like growth factor-1 receptor. *J. Neurosci.* 17:6918–6928.

Delbono, O., and E. Stefani. 1993a. Calcium current inactivation in denervated rat skeletal muscle fibers. *J. Physiol. (Lond.).* 460:173–183.

Delbono, O., and E. Stefani. 1993b. Calcium transients in single mammalian skeletal muscle fibers. *J. Physiol. (Lond.).* 463:689–707.

Dulhunty, A. F., and P. W. Gage. 1983. Asymmetrical charge movement in slow- and fast-twitch mammalian muscle fibers in normal and paraplegic rats. *J. Physiol. (Lond.).* 341:213–231.

Finch, E. A., and G. J. Augustine. 1998. Local calcium signalling by inositol-1,4,5-trisphosphate in Purkinje cell dendrites. *Nature.* 396: 753–756.

Garcia, J., and K. G. Beam. 1994. Relationship of calcium transients to calcium currents and charge movements in myotubes expressing skeletal and cardiac dihydropyridine receptors. *J. Gen. Physiol.* 103:125–147.

Garcia, J., K. McKinley, S. H. Appel, and E. Stefani. 1992. Ca^{2+} current and charge movement in adult single human skeletal muscle fibers. *J. Physiol. (Lond.).* 454:183–196.

Garcia, J., and M. F. Schneider. 1993. Calcium transients and calcium release in rat fast-twitch skeletal muscle fibers. *J. Physiol. (Lond.).* 463:709–728.

Gonoi, T., and S. Hasegawa. 1988. Post-natal disappearance of transient calcium channels in mouse skeletal muscle: effects of denervation and culture. *J. Physiol. (Lond.).* 401:617–637.

Hamill, O. P., A. Marty, E. Neher, B. Sakmann, and F. J. Sigworth. 1981. Improved patch-clamp techniques for high-resolution current recording from cells and cell-free membrane patches. *Pflugers Arch. Eur. J. Physiol.* 391:85–100.

Hodgkin, A. L., and A. F. Huxley. 1952. A quantitative description of membrane current and its application to conduction and excitation in nerve. *J. Physiol. (Lond.).* 177:500–544.

Hollingworth, S., and M. W. Marshall. 1981. A comparative study of charge movement in rat and frog skeletal muscle fibers. *J. Physiol. (Lond.).* 321:583–602.

Hollingworth, S. M., M. W. Marshall, and E. Robson. 1990. The effects of tetracaine on charge movement in fast twitch rat skeletal muscle fibers. *J. Physiol. (Lond.).* 421:633–644.

Jackson, M. B. 1992. Cable analysis with the whole-cell patch clamp. *Biophys. J.* 61:756–766.

Jacquemond, V. 1997. Indo-1 fluorescent signals elicited by membrane depolarization in enzymatically isolated mouse skeletal muscle fibers. *Biophys. J.* 73:920–928.

Lamb, G. D. 1986. Asymmetric charge movement in contracting muscle fibers in the rabbit. *J. Physiol. (Lond.).* 376:63–83.

Lamb, G. D., and T. Walsh. 1987. Calcium currents, charge movement and dihydropyridine binding in fast- and slow-twitch muscles of rat and rabbit. *J. Physiol. (Lond.).* 393:595–617.

Meissner, G. 1994. Ryanodine receptor/Ca^{2+} release channels and their regulation by endogenous effectors. *Annu. Rev. Physiol.* 56:485–508.

Melzer, W., A. Herrmann-Frank, and H. C. Luttgau. 1995. The role of Ca^{2+} ions in excitation-contraction coupling of skeletal muscle fibers. *Biochim. Biophys. Acta.* 1241:59–116.

Schneider, M. F. 1994. Control of calcium release in functioning skeletal muscle fibers. *Annu. Rev. Physiol.* 56:463–484.

Shirokova, N., J. Garcia, G. Pizarro, and E. Rios. 1996. Ca^{2+} release from the sarcoplasmic reticulum compared in amphibian and mammalian skeletal muscle. *J. Gen. Physiol.* 107:1–18.

Simon, B. J., and K. G. Beam. 1985. Slow charge movement in mammalian skeletal muscle. *J. Gen. Physiol.* 85:1–19.

Simon, B. J., and D. A. Hill. 1992. Charge movement and SR calcium release in frog skeletal muscle can be related by a Hodgin-Huxley model with four gating particles. *Biophys. J.* 61:1109–1116.

Szentesi, P., V. Jacquemond, L. Kovacs, and L. Csernoch. 1997. Intramembrane charge movement and sarcoplasmic calcium release in enzymatically isolated mammalian skeletal muscle fibers. *J. Physiol. (Lond.).* 505.2:371–384.

Wang, Z.-M., M. L. Messi, M. Renganathan, and O. Delbono. 1999. Insulin-like growth factor-1 enhances rat skeletal muscle charge movement and L-type Ca^{2+} channel gene expression. *J. Physiol. (Lond.).* 516.2:331–341.

Zhao, M., S. Hollingworth, and S. M. Baylor. 1996. Properties of tri- and tetracarboxylate Ca^{2+} indicators in frog skeletal muscle fibers. *Biophys. J.* 70:896–916.